Resource/Short Communication:

Proteomics characterisation of the L929 cell supernatant and its role in BMDM differentiation

Rachel E. Heap[1], José Luis Marín-Rubio[1], Julien Peltier[1], Tiaan Heunis[1], Abeer Dannoura[1], Adam Moore[1], Matthias Trost[1]

[1]Laboratory for Biological Mass Spectrometry, Biosciences Institute, Newcastle University, Newcastle upon Tyne, NE24HH, UK

*Corresponding author:

Matthias Trost, Tel: +44 191 2087009, E-mail: matthias.trost@ncl.ac.uk

Keywords: bone marrow-derived macrophages, L929, secretome, proteomics, differentiation, M-CSF

Abbreviations: BMDM – bone marrow-derived macrophages; FBS – foetal bovine serum; GO – Gene Ontology; iBAQ – Intensity Based Absolute Quantification; LCCM – L929 Cell Conditioned Media; LC-MS – liquid chromatography mass spectrometry; M-CSF – macrophage colony-stimulating factor-1; MIF – macrophage migration inhibitory factor; TEAB – triethyl ammonium bicarbonate; TFA – Trifluoro acetic acid; TMT – tandem mass tag;

Abstract

Bone marrow-derived macrophages (BMDMs) are a key model system to study macrophage biology *in vitro*. Commonly used methods to differentiate macrophages from bone marrow are treatment with either recombinant M-CSF or the supernatant of L929 cells, which secrete M-CSF. However, little is known about the composition of L929 cell conditioned media (LCCM) and how it affects BMDM phenotype. Here, we used quantitative mass spectrometry to characterise the kinetics of protein secretion from L929 cells over a two-week period, identifying 2,193 proteins. While M-CSF is very abundant in LCCM, we identified several other immune-regulatory proteins such as macrophage migration inhibitory factor (MIF), osteopontin and chemokines such as Ccl2 and Ccl7 at surprisingly high abundance levels. We therefore further characterised the proteomes of BMDMs after differentiation with M-CSF, M-CSF + MIF or LCCM, respectively. Interestingly, macrophages differentiated with LCCM induced a stronger anti-inflammatory M1 phenotype that those differentiated with M-CSF. This resource will be valuable to all researchers using LCCM for the differentiation of BMDMs.

Introduction

Murine bone marrow-derived macrophages (BMDMs) are commonly used to study macrophage functions *in vitro* (1). They are preferred over macrophage and monocyte cell lines as they appear to better represent the macrophage phenotype *in vivo* (2, 3). Importantly, any genetic modification incurred at the organism level is translated into *in vitro* experiments and results can subsequently be verified in the original *in vivo* model. In the last 50 years, two macrophage differentiation practices have been extensively used: the addition of recombinant macrophage colony-stimulating factor-1 (M-CSF or CSF1) or the addition of L929 cell-conditioned medium (LCCM) (4-8). L929 is a fibroblast cell line derived from a clone of normal subcutaneous areolar and adipose tissue of a male C3H/An mouse (9, 10). It was found to secrete a macrophage growth factor (11), which was later identified as M-CSF (4). The *CSF1* DNA sequence was also first cloned from L929 cells (12).

In many labs, LCCM is preferred over the addition of recombinant M-CSF as it is cheaper and generates considerably higher numbers of differentiated macrophages, reducing the number of sacrificed animals by 5 to 10-fold (1). However, there remains scepticism in the field over BMDM differentiation utilising L929 supplemented media. This is partially driven by the utilisation of different protocols (2–4), which will likely influence resultant BMDM properties (5). Furthermore, early studies described that L929 medium could induce an interferon-stimulated phenotype in BMDMs, which may then affect results due to macrophage polarisation (6,7). Despite this heterogeneity in differentiation protocols, BMDMs differentiated with LCCM have been utilised widely for studying macrophage biology, such as regulation of antigen presentation by treatment with IL-4, as well as deciphering cell signalling pathways in response LPS treatment (8–10).

The classification and phenotype of M-CSF differentiated macrophages has been well described with respect to their adhesion and cell surface marker expression, however, they have not been compared with alternative differentiation methods (11,12). Therefore, there is a need to characterise BMDM phenotypes under different culture conditions used for

differentiation to determine whether there are significant differences in biological function. Furthermore, despite the characterisation of M-CSF as a significant component of the L929 secretome, the protein content of the L929 secretome remains poorly defined. Consequently, we report in this paper the secretion profile of L929 cells and characterised the influence of LCCM on BMDM phenotype by quantitative mass spectrometry.

Methods

Cells and Materials

L929 fibroblasts (ATCC CCL-1) were purchased from ATCC (Manassas, USA). Dulbecco's Modified Eagle Medium (DMEM), phosphate buffered saline solution (PBS) and foetal bovine serum (FBS) were all purchased from Gibco, Life Technologies (Darmstadt, Germany). L-glutamine and penicillin-streptomycin were purchased from Lonza (Basel, Switzerland). Trypsin-EDTA solution and trifluoroacetic acid (TFA) were purchased from Sigma Aldrich.

Production of L929 cell-conditioned medium (LCCM)

L929 cells were grown for three passages from cryogenic storage before seeding for secretion collection. Cells were seeded in 50 mL of high glucose Dulbecco´s modified eagle medium (DMEM) containing 10 % (v/v) foetal bovine serum (FBS), 1 mM L-glutamine, 100 U/ml penicillin and 100 µg/ml streptomycin at a density of ~6,500 cells per cm^2 of available surface area. Media was carefully removed after seven days of culture and replaced with 50 mL of fresh DMEM media for a subsequent seven days. The two supernatant collections were then combined and sterile filtered before aliquoting into 50 mL falcon tubes and stored at -20°C.

Collection of supernatants for proteomics time course analysis

L929 cells were seeded in six well plates for secretomics analysis at ~6,500 cells per cm^2 cell density and 1 mL of supplemented DMEM media. For secretome collection, cells were first washed twice with warm PBS and one with Opti-MEM supplemented with 1 mM L-glutamine, 100 U/ml penicillin and 100 µg/ml streptomycin. One millilitre of supplemented Opti-MEM

media was added to each well for a maximum of 3 hours before being carefully removed to avoid disturbing adherent cells. Supernatants were centrifuged at 2,000×g, 4°C for 10 min to pellet cell debris. The supernatant was removed and stored in 1.5 mL Eppendorf lo-bind tubes at -80°C.

Protein precipitation of supernatants for proteomic analysis

Using 5 mL lo-bind tubes (Eppendorf), 960 µL of ice-cold methanol was added to ~1 mL of protein supernatant and vortexed briefly before subsequent addition of 160 µL of ice-cold chloroform and thorough mixing. Two and a half mL of ice-cold water was then added to each tube, vortexed and centrifuged at 4,000×g, 4°C for 30 min. The top layer was carefully removed to prevent disruption of the protein layer. A further 500 µL of ice-cold methanol was then added and the solution vortexed thoroughly before transfer to a 1.5 mL lo-bind tube (Eppendorf) followed by centrifugation at 20,000×g, 4 °C for 30 min. The supernatant was then aspirated and the pellet ambient dried.

Culture of bone marrow-derived macrophages (BMDMs)

Bone marrow-derived macrophages (BMDMs) were isolated from femurs and tibiae of wild-type (WT) C57BL/6J mice of 3-5 months of age. The bone marrow cells were treated with red blood cell lysis buffer (155 mM NH_4Cl, 12 mM $NaHCO_3$ and 0.1 mM EDTA) and suspended in 2 mL of un-supplemented Iscove's modified Dulbecco's medium (IMDM) media. Next, bone marrow cells were transferred into one of three different culture conditions of IMDM supplemented with 10% FBS, 1% L-glutamine, 1% pen/strep and either (1) 20% L929 conditioned media, (2) 10 ng/mL of M-CSF or (3) 10 ng/mL of M-CSF and 10 ng/mL of MIF (Invitrogen). After 24 h, cells in suspension were transferred to petri dishes and seeded at 5.0 – 7.5×10^5 cells per dish. Differentiation occurred over 7 days with an additional 2 mL of fresh media being added at 2, 4 and 6 days.

Flow cytometry analysis

Cells were washed twice in FACS buffer (1% BSA, 1% FBS in PBS, pH 7.2) resuspended and incubated for 30 min in FACS buffer supplemented with Fc gamma receptor CD16/CD32

antibodies (ThermoFisher). Cells were then incubated with Alexa fluor 488-conjugated antibodies against F4/80 or rat IgG2a kappa isotype control, allophycocyanin (APC)-conjugated antibodies against CD11c or Armenian hamster IgG isotype control, phycoerythrin (PE)-conjugated antibodies against CD11b or rat IgG2b kappa isotype control at 1:100 dilution in FACS buffer for 30 min in the dark for 4°C. Antibodies were purchased from Invitrogen. For proliferation analyses, the cells were stained with CellTrace™ Violet dye (Invitrogen). Cells were analysed in a FACS Canto II flow cytometer (Becton-Dickinson). The results were analysed using FlowJo V10.

ELISA

BMDMs cultured in either M-CSF or L929 supernatant were treated with 100 ng/mL of LPS. The supernatant was collected after 6 h and centrifuged at 10,000×g for 10 min to remove cell debris. The supernatant was transferred to a new tube and ELISAs for TNF-α, IL-6 and IFN-β (DuoSet mouse ELISA kits from R&D Systems) were performed according to manufacturer's instruction.

Proteomics

Protein extraction, reduction and alkylation

For both L929 cell-free supernatants and BMDM cell pellets three biological replicates were collected. Precipitated L929 secretions were resuspended in 8M Urea, 50 mM triethyl ammonium bicarbonate (TEAB) pH 8.5, whereas BMDM cell pellets were lysed in 5% SDS, 50 mM TEAB pH 7.55. Protein quantification was determined using the BCA Protein Assay Kit (Pierce Protein). Fifty µg of each sample was reduced by addition of TCEP to a final concentration of 10 mM for 30 min at room temperature followed by alkylation with 10 mM iodoacetamide for 30 min at room temperature in the dark.

In-solution protein digestion of L929 secretomes

Samples were diluted to 1 M urea using 50 mM TEAB pH 8.5 and digested overnight at 37°C by adding porcine trypsin (1:50, w/w) (Pierce). Peptides were then acidified, desalted and

concentrated using C18 SPE Macro Spin Columns (Harvard Apparatus). Peptides were then dried under vacuum.

S-Trap protein digestion for BMDM proteomes

Samples were acidified by addition of 2.5 µL of 12% phosphoric acid and diluted with 165 µL of S-trap binding buffer (90% MeOH, 100 mM TEAB, pH 7.1). The acidified samples were then loaded onto the S-trap spin column (ProtiFi, USA) and centrifuged at 4,000×g for 1 min. Columns were washed five times with S-trap binding buffer before addition of porcine trypsin (1:20) (Pierce) in 25 µL of 50 mM TEAB to the column. Samples were incubated at 47°C for 2 h. Peptides were eluted by washing the column with 50 mM TEAB, pH 8.0 (40 µL), followed by 0.2% FA (40 µL) and finally 0.2% FA, 50% MeCN (40 µL). Peptides were then dried under vacuum.

TMT 10-plex labelling of BMDM cellular proteome samples

Isobaric labelling of peptides was performed using the 10-plex tandem mass tag (TMT) reagents (Thermo-Fisher). TMT reagents (0.8 mg) were resuspended in 41 µL of acetonitrile, and 10 µL was added to the corresponding samples that were previously resuspended in 50 µL of 50 mM TEAB, pH 8.5. After 1 hour incubation at room temperature the reaction was quenched by addition of 4 µL of 5% hydroxylamine. Labelled peptides were then combined and acidified with 200 µL of 1% TFA (pH ~ 2) and concentrated using C18 SPE on Sep-Pak cartridges (Waters). Mixing ratios of each channel and labelling efficiency was tested by injection of a small pool of each channel on a Fusion Lumos Tribid mass spectrometer. Each TMT-labelled sample was tested separately to ensure a labelling efficiency >95%.

High-pH reversed-phase liquid chromatography fractionation

The combined TMT-labelled peptides were fractionated by high-pH reversed-phase (HPRP) liquid chromatography. Labelled peptides were solubilized in 20 mM ammonium formate (pH 8.0) and separated on a Gemini C18 column (250 × 3 mm, 3 µm C18 110 Å pore size; Phenomenex). Using a DGP-3600BM pump system equipped with a SRD-3600 degasser (Thermo-Fisher), a 40 min gradient from 1 to 90% acetonitrile (flow rate of 0.25 mL/min)

separated the peptide mixtures into a total of 40 fractions. The 40 fractions were concatenated into 10 samples, dried under vacuum centrifugation and resuspended in 0.1% (v/v) TFA for LC-MS/MS analysis.

LCCM label-free proteomics analysis

Peptide samples were separated on an Ultimate 3000 RSLC system (Thermo Scientific) with a C18 PepMap, serving as a trapping column (2 cm x 100 µm ID, PepMap C18, 5 µm particles, 100 Å pore size) followed by a 50 cm EASY-Spray column (50 cm x 75 µm ID, PepMap C18, 2 µm particles, 100 Å pore size) (Thermo Scientific). Buffer A contained 0.1% formic acid (FA) and Buffer B 80% MeCN, 0.1% FA. Peptides were separated with a linear gradient of 1-35% (Buffer B) over 120 minutes followed by a step from 35-90% MeCN, 0.1% FA in 0.5 min at 300 nL/min and held at 90% for 4 min. The gradient was then decreased to 1% Buffer B in 0.5 minutes at 300 nL/min for 10 min. Mass spectrometric analysis was performed on an Orbitrap QE HF mass spectrometer (Thermo Scientific) operated in “Top20” data dependant mode in positive ion mode. Full scan spectra were acquired in a range from 400 m/z to 1,500 m/z, at a resolution of 120,000 (at 200 m/z), with an automatic gain control (AGC) target of $1x10^6$and a maximum injection time of 50 ms. Charge state screening was enabled to exclude precursors with a charge state of 1. For MS/MS analysis, the minimum AGC target was set to 5,000 and the most intense precursor ions were isolated with a quadrupole mass filter width of 1.6 *m/z* and 0.5 *m/z* offset. Precursors were subjected to HCD fragmentation that was performed using a one-step collision energy of 25%. MS/MS fragment ions were analysed in the Orbitrap mass analyser with a 15,000 resolution at 200 *m/z*.

Proteomics analysis of TMT-labelled BMDMs

Peptide samples were separated on an Ultimate 3000 RSLC system (Thermo Scientific) with a C18 PepMap, serving as a trapping column (2 cm × 100 µm ID, PepMap C18, 5 µm particles, 100 Å pore size) followed by a 50 cm EASY-Spray column with a linear gradient consisting of (2.4–28% MeCN, 0.1% FA) over 180 min at 300 nL/min. Mass spectrometric analysis was performed on an Orbitrap Fusion Lumos Tribrid mass spectrometer (Thermo-Fisher Scientific)

operated in data dependent, positive ion mode. Full scan spectra were acquired in the range of 400 *m/z* to 1,500 *m/z*, at a resolution of 120,000, with an automatic gain control (AGC) target of $3x10^5$ ions and a maximum injection time of 50 ms. The 12 most intense precursor ions were isolated with a quadrupole mass filter width of 1.6 m/z and collision induced dissociation (CID) fragmentation was performed in one-step collision energy of 35% and 0.25 activation Q. Detection of MS/MS fragments was acquired in the linear ion trap in rapid scan mode with an AGC target of 10,000 ions and a maximum injection time of 40 ms. Quantitative analysis of TMT-tagged peptides was performed using FTMS3 acquisition in the Orbitrap mass analyser operated at 60,000 resolution, with an AGC target of 100,000 ions and maximum injection time of 120 ms. Higher-energy collision induced dissociation (HCD fragmentation) on MS/MS fragments was performed in one-step collision energy of 55% to ensure maximal TMT reporter ion yield and synchronous-precursor-selection (SPS) was enabled to include 10 MS/MS fragment ions in the FTMS3 scan.

Data analysis

Protein identification and label free quantification for the L929 secretome data set was performed using MaxQuant Version 1.6.2.6 (13). Trypsin/P set as enzyme; stable modification carbamidomethyl (C); variable modifications Oxidation (M), Acetyl (Protein N-term), Deamidation (NQ), Gln & Glu to pyro-Glu; maximum 8 modifications per peptide, and 2 missed cleavage. Searches were conducted using the mouse Uniprot database plus isoforms (downloaded 19.07.2018; 25,192 sequences) plus common contaminants. Identifications were filtered at a 1% FDR at the peptide level and protein level, accepting a minimum peptide length of 5. Quantification was performed using razor and unique peptides and required a minimum count of 2. “Re-quantify” and “match between runs” were enabled. LFQ protein intensities were used for downstream analyses (14).

Protein identification for the TMT labelled total proteome data set was performed using MaxQuant Versions 1.6.2.6 with Reporter ion MS2 selected as experiment type (13). Trypsin/P set as enzyme; stable modification carbamidomethyl (C); variable modifications Oxidation (M),

Acetyl (Protein N-term), Deamidation (NQ), Gln & Glu to pyro-Glu and quantitation of labels with 10 plex TMT on N-terminal or lysine with a reporter mass tolerance of 0.003 Da. Two missed cleavages and a maximum of 8 modifications per peptide were set. Match between runs was enabled for this search. Searches were conducted using the mouse Uniprot database plus isoforms (downloaded 19.07.2018; 25,192 sequences) plus common contaminants. Identifications were filtered at a 1% FDR at the peptide level and protein level, accepting a minimum peptide length of 5. Quantification of proteins refers to the razor and unique peptides, and required a minimum count of 2. Normalized reporter ion intensities were extracted for each of the 9 channels were used for downstream analyses. A total of 6,724 proteins were identified of which 5,591 were quantified.

Statistical Analysis

Statistical analyses were performed in Perseus (v1.6.0.7 - v1.6.6.0) (14). For both the label free and TMT data sets, contaminants and reverse hits were removed from the data sets prior to analyses.

For the L929 secretome data set, the Log_2 normalised LFQ protein intensities were used for subsequent analysis. The dataset was first filtered to only include proteins that were identified in 2 out of 3 of the biological replicates for each day to yield a data set of 1,582 confidently identified proteins. To extract regulated proteins across the total time course an ANOVA T-test was performed with a Benjamini-Hochberg FDR correction of 0.05 and 1,128 proteins were identified as regulated. These proteins were Z-scored by row and the groups mean averaged before hierarchical clustering was performed with Euclidian distancing on the rows only (27 clusters and 10 maximal number of iterations).

For analysis of the TMT total proteome data set, the Log_2 normalised reporter ion intensities were used for subsequent analysis. The dataset was filtered for proteins that were identified in 3 of the 9 groups which gave a data set of 5,569 confidently identified proteins. Two sample T-tests were applied between L929 and MIF, L929 vs MCSF and M-CSF vs MIF with a Benjamini-Hochberg FDR correction of 0.05.

Data availability

The mass spectrometry proteomics data have been deposited to the ProteomeXchange [15] Consortium via the PRIDE [16] partner repository with the dataset identifier PXD021026 Reviewers can access it through the Username: reviewer47540@ebi.ac.uk and the Password: cEZLfJl0

Results

Kinetic profiling of the L929 secretome by proteomics

In order to understand the role of L929 cell-conditioned medium (LCCM) on macrophage differentiation, we first characterised LCCM using a proteomics approach. In most protocols, L929 cells are initially seeded and not further passaged (17). The collection of LCCM is then typically performed between 7 and 14 days, with some protocols combining both time points to generate potent differentiation media. Therefore, we characterised the secretion profile of L929 fibroblasts over the two-week time period by sampling at 3, 7, 10 and 14 days (**Figure 1A**). L929 fibroblasts were seeded at ~6,500 cells per cm^2 as would be used for LCCM collection. Cells were grown over 14 days and bright field light microscopy was used to visualise the progression of cell confluency at days 3, 7, 10 and 14 (**Supplementary Figure 1**), showing increasing confluency and morphology changes over time.

Label-free proteomics analysis of the four time points of LCCM identified 2,549 proteins, with 2,193 being robustly identified with 2 or more unique+razor peptides (**Supplementary Table 1**). Taking the data set as a whole, gene ontology (GO) enrichment analysis identified a highly significant enrichment of extracellular exosomes as well as cytosolic protein groups (**Figure 1B**). The top three proteins identified from the secretome comprised of fibronectin, actin and collagen alpha-type-2, which is unsurprising for fibroblast cells as they are known to secrete high levels of these extracellular matrix proteins (18,19). We used Intensity Based Absolute Quantification (iBAQ) (20), which enables an estimate of absolute quantitation of protein abundance, to generate a list of selected 20 proteins that could influence subsequent BMDM phenotype (**Table 1**).

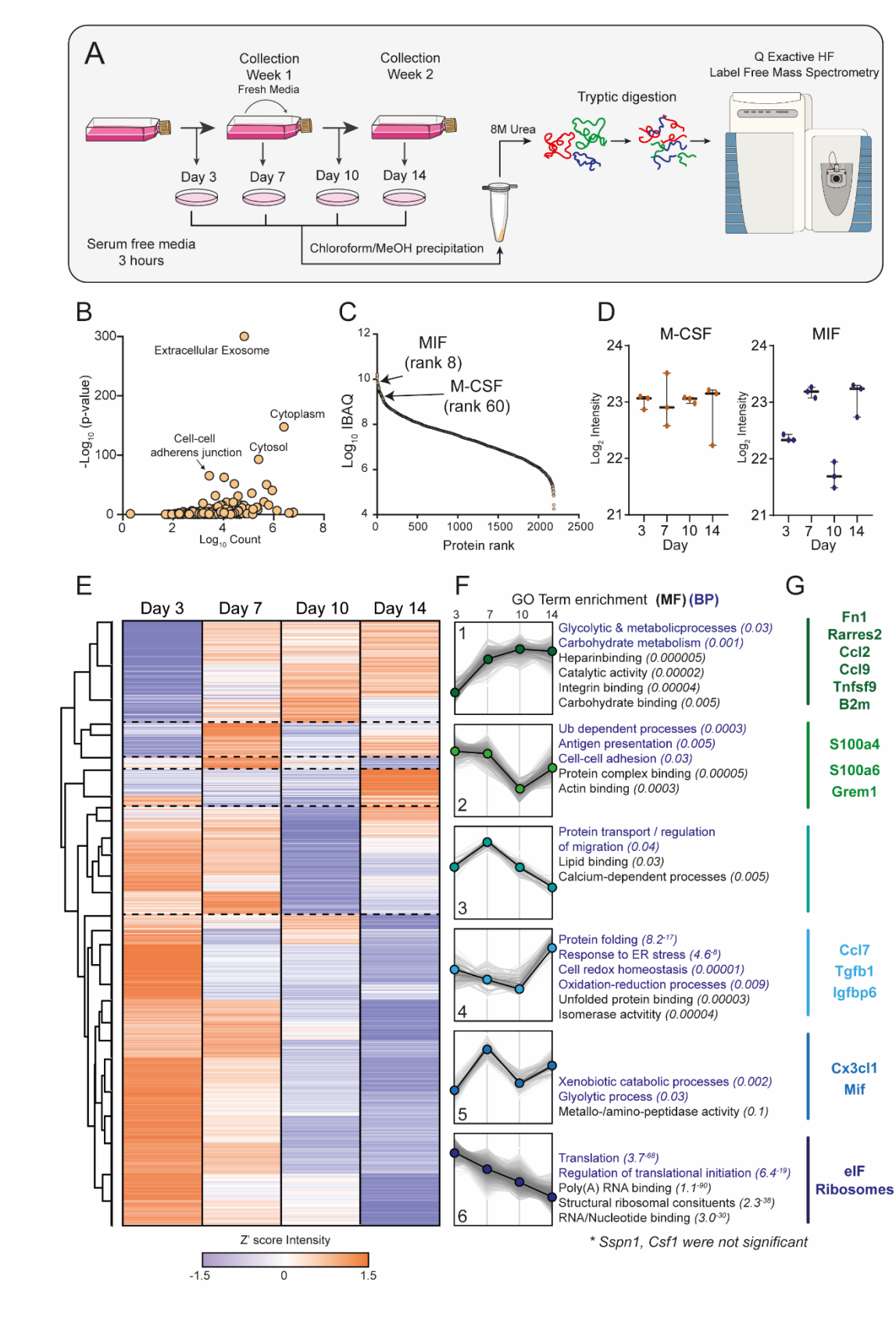
A
Collection Week 1
Fresh Media
Collection Week 2
Q Exactive HF
Label Free Mass Spectrometry
Tryptic digestion
8M Urea
Day 3
Day 7
Day 10
Day 14
Serum free media 3 hours
Chloroform/MeOH precipitation
B
Extracellular Exosome
Cytoplasm
Cell-cell adherens junction
Cytosol
-Log10 (p-value)
Log10 Count
C
MIF (rank 8)
M-CSF (rank 60)
Log10 IBAQ
Protein rank
D
M-CSF
MIF
Log2 Intensity
Day
E
Day 3
Day 7
Day 10
Day 14
Z' score Intensity
-1.5
0
1.5
F
GO Term enrichment (MF) (BP)
Glycolytic & metabolicprocesses (0.03)
Carbohydrate metabolism (0.001)
Heparinbinding (0.000005)
Catalytic activity (0.00002)
Integrin binding (0.00004)
Carbohydrate binding (0.005)
Ub dependent processes (0.0003)
Antigen presentation (0.005)
Cell-cell adhesion (0.03)
Protein complex binding (0.00005)
Actin binding (0.0003)
Protein transport / regulation of migration (0.04)
Lipid binding (0.03)
Calcium-dependent processes (0.005)
Protein folding (8.2-17)
Response to ER stress (4.6-8)
Cell redox homeostasis (0.00001)
Oxidation-reduction processes (0.009)
Unfolded protein binding (0.00003)
Isomerase actvitity (0.00004)
Xenobiotic catabolic processes (0.002)
Glyolytic process (0.03)
Metallo-/amino-peptidase activity (0.1)
Translation (3.7-68)
Regulation of translational initiation (6.4-19)
Poly(A) RNA binding (1.1-90)
Structural ribosomal consituents (2.3-38)
RNA/Nucleotide binding (3.0-30)
G
Fn1
Rarres2
Ccl2
Ccl9
Tnfsf9
B2m
S100a4
S100a6
Grem1
Ccl7
Tgfb1
Igfbp6
Cx3cl1
Mif
eIF
Ribosomes
* Sspn1, Csf1 were not significant

280

Figure 1. L929 cell conditioned-media proteome. (A) Workflow. Graphical representation of the collection of L929 supernatant over 14 days and the corresponding secretome collections for proteomic analysis. (B) Gene Ontology (GO) analysis of proteins identified in LCCM shows enrichment of exosomes and cytoplasmic proteins. (C) Log10 intensity-based absolute quantification (iBAQ) values ranking of proteins from the L929 secretome showing positions of MIF and M-CSF. (D) Z'-scored heat map of ANOVA significant proteins across the sampling days. (E) Six distinct cluster profiles that show different secretion patterns over time with purple dots indicating down and orange dots up regulation. (F) Associated molecular function and biological process GO terms for the six cluster profiles. (G) Intensity levels of M-CSF (CSF1) and MIF in LCCM over the two-week growth period of L929 cells. Error bars in (E) represent standard deviation.

Table 1: Twenty selected proteins identified in L929 CM with iBAQ ranking (known cytokines and chemokines in bold)

iBAQ Rank	Uniprot Accession	Gene names	Protein names	# ident. Peptides	Log10 iBAQ
1	P60710	Actb	Actin, cytoplasmic 1 (Beta-actin)	28	10.23
2	P11276	Fn1	Fibronectin (FN)	152	10.20
3	P21460	Cst3	Cystatin-C (Cystatin-3)	9	10.15
4	P16045	Lgals1	Galectin-1	12	10.08
5	**Q9DD06**	**Rarres2**	**Retinoic acid receptor responder protein 2 (Chemerin)**	**17**	**10.04**
6	P01887	B2m	Beta-2-microglobulin	7	9.88
7	**P34884**	**Mif**	**Macrophage migration inhibitory factor (MIF)**	**7**	**9.85**
8	P47879	Igfbp4	Insulin-like growth factor-binding protein 4	17	9.81
9	**P10923**	**Spp1**	**Osteopontin**	**9**	**9.75**
10	P07091	S100a4	Protein S100-A4 (Metastasin)	7	9.75
40	P14069	S100a6	Protein S100-A6 (Calcyclin)	10	9.38
47	**Q03366**	**Ccl7**	**C-C motif chemokine 7**	**4**	**9.32**
54	**P07141**	**Csf1**	**Macrophage colony-stimulating factor 1**	**19**	**9.23**
64	**P10148**	**Ccl2**	**C-C motif chemokine 2**	**5**	**9.19**
221	**P12850**	**Cxcl1**	**Growth-regulated alpha protein (C-X-C motif chemokine 1)**	**3**	**8.57**
263	**O35188**	**Cx3cl1**	**Fractalkine (C-X3-C motif chemokine 1)**	**10**	**8.48**
489	**P51670**	**Ccl9**	**C-C motif chemokine 9**	**4**	**8.09**
496	**O70326**	**Grem1**	**Gremlin-1**	**8**	**8.08**
905	**P04202**	**Tgfb1**	**Transforming growth factor beta-1 proprotein**	**11**	**7.62**
1012	**P41274**	**Tnfsf9**	**Tumor necrosis factor ligand superfamily member 9**	**4**	**7.49**

In the top 100 most abundant proteins, we identified Chemerin (Rarres2), MIF, Osteopontin, Ccl7, M-CSF and Ccl2 as potential active immune-modulatory proteins in LCCM (**Figure 1C; Table 1**). Chemerin is an adipokine (21), which has been shown to serve as chemo-attractant for cells of the innate immune system (22). It has been shown to decrease IL-10 production in anti-inflammatory macrophages (23). Macrophage migration inhibitory factor (MIF) was

identified as a highly abundant component of the L929 secretion and is a cytokine that has been shown to inhibit human monocyte and T cell migration (24). MIF has further been shown to regulate inflammation via direct and indirect effects modulating the release of multiple cytokines, including TNF-α, IFN-γ, IL-2, IL-6, and IL-8 (25). Osteopontin is a cytokine mediating innate-adaptive immune crosstalk and acts on macrophages by upregulating IL-12 production. It also acts on T-helper cells, inducing Th17 polarization (26). Ccl7 and Ccl2 are potent chemokines particularly attracting blood monocytes to sites of inflammation (27). L929 cells also secrete TGF-β (at rank 905), but at ~40-fold and ~170-fold lower abundance than M-CSF and MIF, respectively.

Looking at the total secretome, we further investigated if specific functional groups of proteins were changing at specific times during the 14 days of LCCM production. Analysis of 1,128 ANOVA significant protein groups showed distinct patterns in protein secretion rates over time, and that processes such as translation reduced over time while glycolytic and metabolic processes were increasing (**Figure 1D-E; Supplementary Figure 2**). The secretion levels of some of the previously highlighted cytokines and chemokines were variable over the 14-day period of LCCM production (**Figure 1D-E**). The rate of M-CSF secretion was overall consistent throughout the two-week L929 secretion time. The rate of MIF secretion correlated with depletion of nutrients within the media, as rates decreased two-fold after addition of fresh media. This could imply that MIF is increasingly secreted with a shift in metabolism when less nutrients are available.

Taken together, these data provide a comprehensive list of proteins that are secreted by L929 fibroblasts over a two-week time period. Within this data set, M-CSF was expectedly identified as being a highly abundant secreted protein, however, other immunomodulatory proteins such as MIF were also identified as a highly secreted protein, which may influence subsequent BMDM differentiation.

Characterising the influence of culture conditions on BMDM proteomes

Next, we evaluated how proteomes of BMDMs changed when they were differentiated with 20% LCCM or recombinant M-CSF. As MIF was the highest secreted immunomodulatory cytokine, we deemed it necessary to also explore whether MIF impacted BMDM differentiation. Therefore, three culture conditions were defined: 10 ng/mL of M-CSF, 10 ng/mL of MIF + 10 ng/mL of M-CSF and 20% LCCM. The concentration of 10 ng/mL was chosen for M-CSF as this is the most widely reported differentiation concentration (28,29). Furthermore, the LCCM iBAQ data indicated that MIF (12 kDa) was about five times more abundant than M-CSF (60 kDa), thus indicating similar total amounts of both proteins in the L929 supernatant. The LCCM collection for BMDM differentiation was performed in tandem to the secretome proteomics analyses. We pooled the three LCCM replicates for these experiments, thus the protein composition described is an accurate representation of the differentiation media.

For proteomics analysis, the biological replicates from three different mice of each culture condition were first digested and then labelled by TMT 10-plex (**Figure 2A**). This enabled pooling of all samples and offline-HPLC high-pH reversed phase (HPRP) peptide separation to enable deeper proteome analysis as peptides are orthogonally separated. In total, 4,296 protein groups were identified with 4,279 quantified with 2 razor + unique peptides. Interestingly, there were no significant differences in protein expression between BMDMs cultured with M-CSF ± MIF, thus implying that there is little impact of MIF on M-CSF differentiated macrophages. Conversely, about 150 differential proteins were identified between LCCM differentiated BMDMs and the two other culture conditions (**Figure 2B-C**).

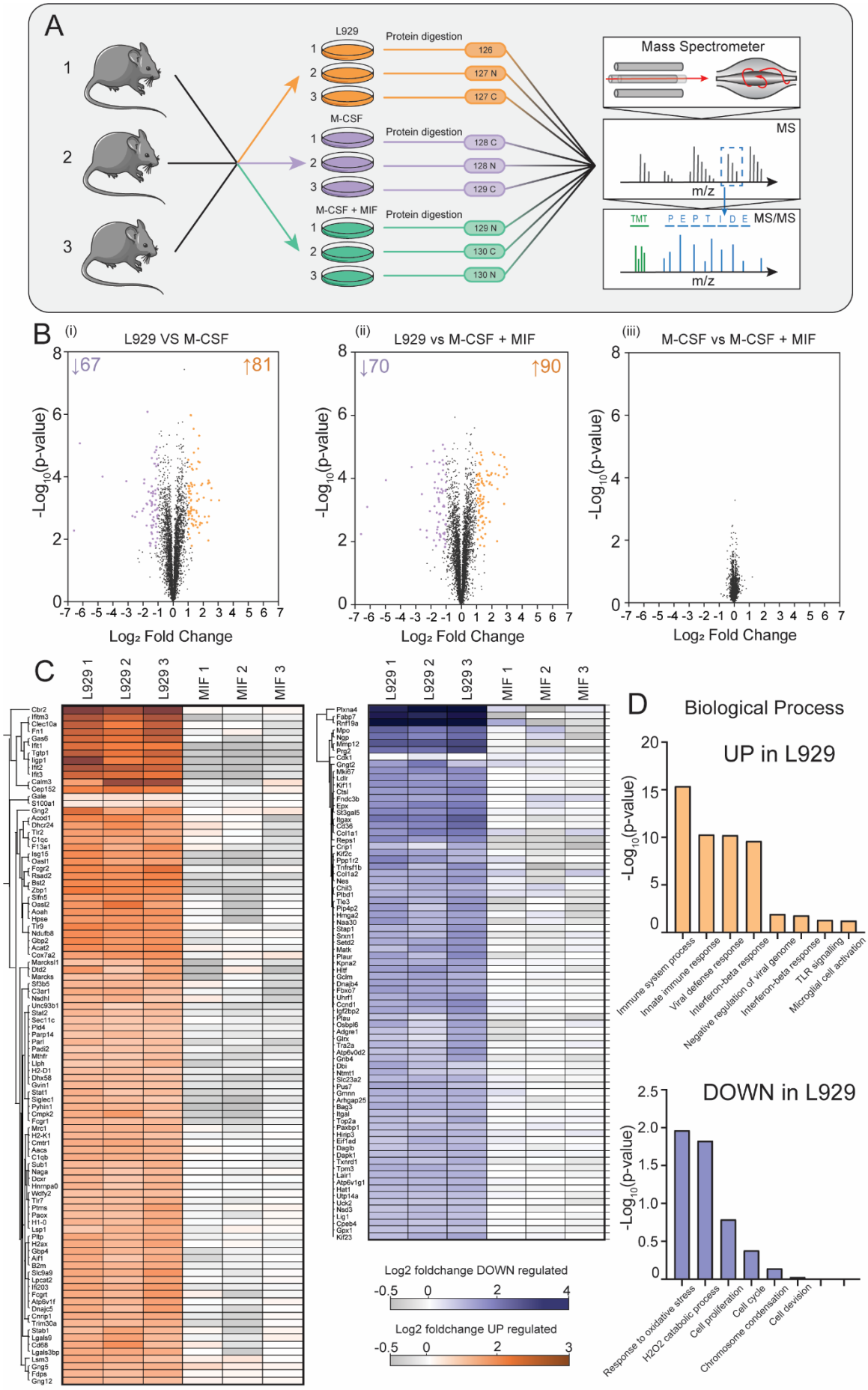
A
L929
M-CSF
M-CSF + MIF
Protein digestion
126
127 N
127 C
128 C
128 N
129 C
129 N
130 C
130 N
Mass Spectrometer
MS
m/z
TMT
P E P T I D E
MS/MS
B
(i) L929 VS M-CSF
(ii) L929 vs M-CSF + MIF
(iii) M-CSF vs M-CSF + MIF
↓67
↑81
↓70
↑90
-Log10(p-value)
Log2 Fold Change
C
L929 1
L929 2
L929 3
MIF 1
MIF 2
MIF 3
Log2 foldchange DOWN regulated
Log2 foldchange UP regulated
D
Biological Process
UP in L929
Immune system process
Innate immune response
Viral defense response
Interferon-beta response
Negative regulation of viral genome
Interferon-beta response
TLR signalling
Microglial cell activation
DOWN in L929
Response to oxidative stress
H2O2 catabolic process
Cell proliferation
Cell cycle
Chromosome condensation
Cell devision

Figure 2. Proteome analysis of BMDMs differentiated with LCCM, M-CSF or M-CSF + MIF. (A) Workflow of the proteomics experiment. Biological triplicates of BMDMs differentiated with LCCM or M-CSF or MCSF + MIF were lysed, proteins digested and labelled with isotopic TMT labels. Proteins were fractionated and analysed by quantitative mass spectrometry. (B) Volcano plots of the three culture conditions compared showing differential proteins with respect to BMDM populations. (C) Heatmap of the Log2 fold change of LCCM vs M-CSF + MIF conditions for all of the proteins that were identified as significantly changing between LCCM vs M-CSF + MIF culturing conditions. (L1-3: replicates differentiated with LCCM; M1-3: replicates differentiated with M-CSF) (D) Biological processes GO enrichment of proteins that were up- or down-regulated in LCCM-differentiated BMDMs with respect to M-CSF + MIF.

GO term enrichment of the differentially regulated proteins showed significant enrichment with respect to biological processes (**Figure 2D**). Interestingly, these data indicate that BMDMs grown in L929 supplemented media have a heightened interferon and innate immune response compared with M-CSF ± MIF cultured BMDMs. Conversely, BMDMs grown in L929 supernatant show down-regulation of response to oxidative stress, cell division and mitotic machinery. These differential proteins were plotted using Log_2 fold change of the TMT reporter ion intensities and hierarchical clustering using Euclidean distancing between L929 and M-CSF + MIF culture conditions showing good clustering of up and down-regulated proteins that were highly consistent over three biological replicates.

To further investigate phenotypic differences between the three BMDM populations, we analysed cell surface receptor expression and the host response upon LPS stimulation. Firstly, three cell surface markers was evaluated using flow cytometry: F4/80, a widely used murine marker of macrophage and dendritic cell populations; CD11b, integrin alpha M (ITGAM), which is highly expressed by myeloid lineage cells, including neutrophils, monocytes, macrophages, and microglia; and CD11c, integrin alpha X (ITGAX), which is used as a dendritic cell marker (30–32).

Next, we tested if the BMDMs differed in expression of F4/80, CD11b and CD11c. While F4/80 and CD11b were expressed at similar levels between the BMDM populations, there were significant differences in the expression of CD11c (**Figure 3A**). Measurement of CD11c showed that there were about twice as many CD11c positive cells in BMDMs cultured with M-

CSF compared to LCCM. This suggests that M-CSF induces more dendritic cell-like features than L929 supernatant.

As the proteomics data showed a difference in proteins involved in innate immune responses and a possible interferon phenotype, we sought to assess the differences in cytokine secretion after a pro-inflammatory stimulation with 100 ng/mL of LPS for six hours. We measured the secretion of TNF-α, IL-6 and IFN-β by ELISA. BMDMs cultured with M-CSF presented a significant reduction in TNF-α, IL-6 and IFN-β compared to L929 conditioned media (**Figure 3B**). These results indicate that LCCM induces a stronger polarisation towards a pro-inflammatory phenotype than M-CSF.

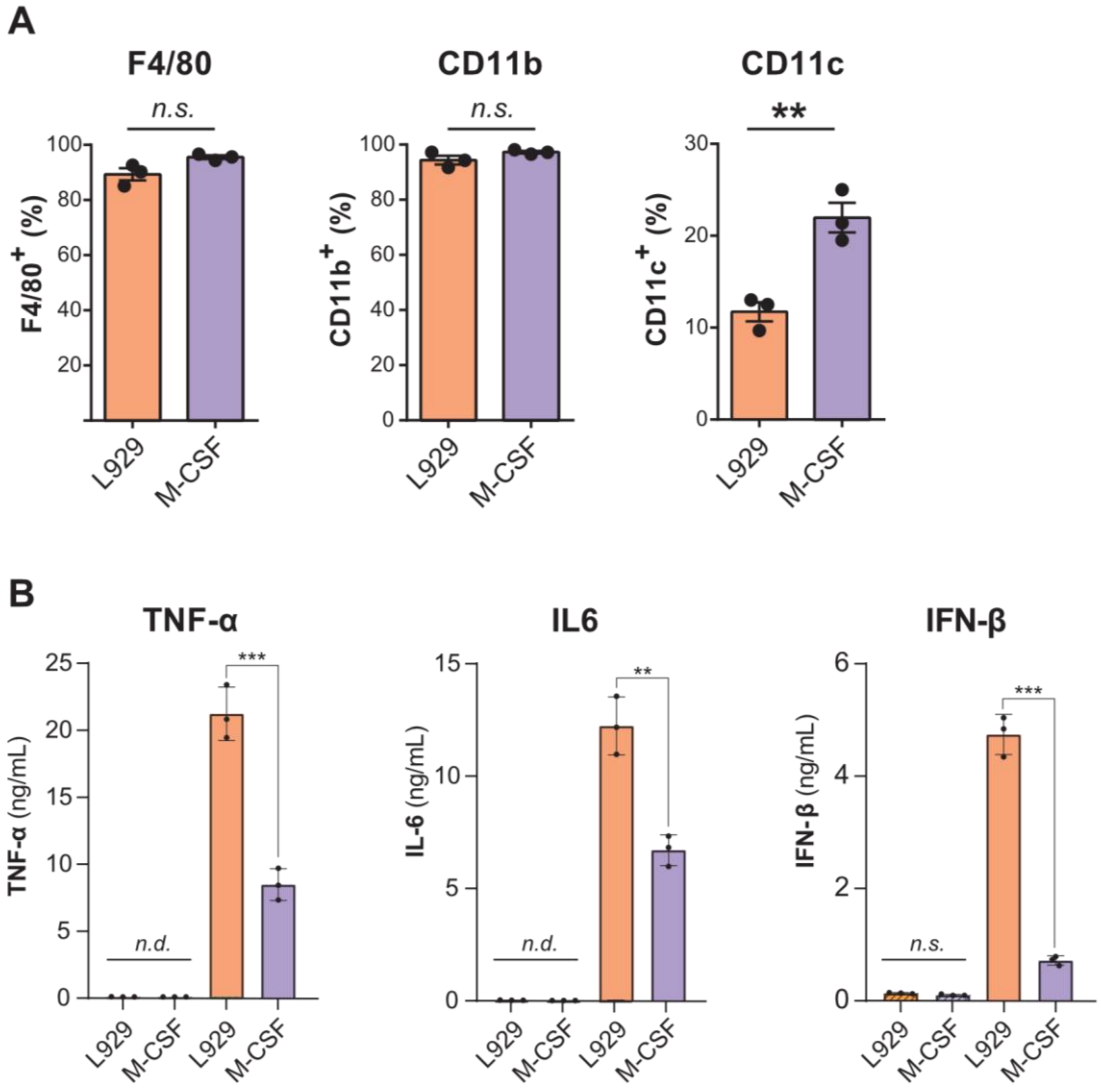

Figure 3. Characterisation of BMDMs differentiated by L929 supernatant and M-CSF. (A) Flow cytometry analysis of CD11b as well as F4/80 and CD11c markers in BMDM cells cultured with L929 conditioned media and M-CSF. (B) ELISAs of TNF-α, Interleukin-6 (IL6) and Interferon-β (IFN-β) of different macrophage populations in response to treatment with 100 ng/mL LPS for 6 h show that LCCM-differentiated macrophages have enhanced immune responses compared to M-CSF-differentiated macrophages. Error bars represent standard deviation. Significance was measured by Student's t-test. P-value: * > 0.05, ** > 0.01 and *** > 0.001. n.d., not detected. n.s., not significant.

Taken together, these data show that the differentiating agent used induces slightly different BMDM phenotypes with respect to their proteomes and biological functions. Therefore, it is important to consider the biological ramifications that result from the different BMDM differentiation strategies and resultant *in vitro* biological outcome.

Discussion

Bone marrow-derived macrophages are primary cells derived from the isolation of haemopoietic stem cells from mammalian femurs and tibia and differentiated *in vitro*. These macrophages are particularly important for understanding biological functions and complex signalling cascades involved in the immune response as they provide the best models for *in vitro* experiments.

Initially, macrophage colony stimulating factor (M-CSF) was identified as the main driver of primary macrophage differentiation and was introduced *in vitro* as an active differentiation agent. However, in more recent years the supplementation of differentiation media with the cell-free supernatant of L929 fibroblasts has become favourable as it is cheaper and relatively simple to produce in-house. L929 fibroblasts were isolated from connective tissue and have been shown to produce and secrete high levels of M-CSF. This may be physiologically relevant to this cell type, as fibroblasts are a major component of connective tissue and play a critical role in wound healing and recruitment of macrophages (33). Furthermore, fibroblasts secrete cytokines and chemokines to modulate macrophage behaviour and the inflammatory response. Therefore, the production of M-CSF is necessary for the initial recruitment of

macrophages to sites of injury (34). However, the secretion of fibroblasts is much more complex than pure recombinant M-CSF. A recent paper showed that LCCM changed the metabolism of macrophages to a higher glycolytic state compared to macrophages differentiated with M-CSF (35). In contrast to our data, they also showed that M-CSF differentiation was leading to more TNF-α secretion upon LPS activation, while IL6 was strongly enhanced in LCCM differentiated BMDMs. One difference between our data and this paper could be that we sterile-filtered the LCCM, thereby removing apoptotic bodies which may by phagocytosed by macrophages and affect overall macrophage metabolism.

The primary aim of this study was to describe the protein composition of the L929 supernatant across the collection time period. Here, 2,193 proteins were robustly identified over the two-week time course with different expression rates. Interestingly, the top 100 iBAQ proteins contributed towards more than 60% of the total protein content with M-CSF being highly expressed. However, other cytokines such as macrophage migration inhibitory factor (MIF) were also identified alongside the chemo-attractants Chemerin and Osteopontin and the two chemokines Ccl7 and Ccl2. This may indicate that the L929 supernatant may induce a specific activation state during the differentiation on BMDMs. However, secretion of both IFN-γ and IFN-β were measured by ELISA for all four sampling conditions and neither of the two interferons were detectable (data not shown), thus disputing previous studies that reports the production of type 1 interferons by L929 fibroblasts during the supernatant collection period (6).

Utilising flow cytometry, biochemistry and total proteome analysis, we were able to assess the phenotypic differences between the three BMDM populations. There was no significant difference in total protein expression between BMDMs cultured with or without the presence of MIF, which was surprising as it has previously been described as a mediator of host defence (36). This implies that MIF cannot solely influence macrophage phenotype and is likely to act in tandem with other cytokines that are released during injury or infection to coordinate a pro-inflammatory response.

The total proteome of BMDMs differentiated using L929 supplementation had a distinct phenotype compared with recombinant M-CSF or M-CSF + MIF. The 109 differential proteins that GO term enrichment analysis revealed were either involved in cell cycle/mitosis or the innate immune response. L929-differentiated BMDMs showed much higher expression of proteins involved in the interferon and immune response such as interferon induced proteins IFIT1, IFIT3, IFITM2, IFITM3 and ISG15. They also expressed higher levels of the Toll-like receptors 2, 7 and 9. As well as this, L929 differentiated BMDMs show decreased protein expression of cell division and cell cycle proteins such as cyclin-A2, spindle and centromere proteins SPDLY and INCE compared to pure M-CSF differentiation. Consequently, this implies that factors in the L929 supernatant may affect the cell cycle, perhaps through faster terminal differentiation. This is also supported by the considerable higher number of BMDMs obtained after seven days of differentiation. It also implies that differentiation with LCCM generates a population of macrophages that are more mature than those differentiated purely with M-CSF.

Following this, flow cytometry analysis of surface expressed markers correlated with our proteomic data. While all populations showed high surface expression levels of F4/80 and CD11b, the marker CD11c, which is traditionally used for dendritic cells, was more highly expressed on macrophages differentiated with M-CSF. This indicates that M-CSF differentiated macrophages are possibly more dendritic cell-like.

To assess the pro-inflammatory response of the three BMDM populations, the secretion of pro-inflammatory cytokines was measured after stimulation with LPS. Three cytokines were measured in response to LPS: TNF-α, IL-6 and IFN-β, which cover the classical NF-κB pro-inflammatory and type I interferon responses. At basal levels, with no treatment, there were undetectable levels of TNF-α and IL-6, thus implying that all BMDM populations are not pro-inflammatory stimulated throughout the differentiation. There were detectable, but very low levels of IFN-β secretion under basal conditions. However, these were not significantly different between the conditions. This in turn shows that despite the variety of proteins present in the L929 supernatant, they do not induce *per se* an interferon activated state in BMDMs.

Upon stimulation, BMDMs that were differentiated by LCCM appeared primed and showed a significantly increased pro-inflammatory response by secreting higher levels of the three cytokines measured. This was particularly pronounced with IFN-β, where levels were elevated five-fold in response to LPS compared to M-CSF.

Inclusion of MIF as a differentiation agent resulted in a negligible difference in cellular phenotype with respect to total proteome, cytokine secretion and protein cell surface marker expression. Overall, our data shows that differentiation with L929 supplemented media generates a population of cells that is less naïve than M-CSF or M-CSF + MIF alone. From a biological perspective this is expected, as *in vivo* induction of macrophage differentiation would likely be initiated by cellular secretion of multiple factors in response to injury or pathogenic infection. Fibroblasts play a significant role in the recruitment of macrophages and their migration towards the site of infection or injury.

Taken together, it is possible to conclude that M-CSF is a driving component of BMDM differentiation, but other factors secreted by L929 fibroblasts influence the resulting cellular phenotype. Further exploration of these factors would be necessary to understand the subtleties in BMDM differentiation and what induces the described phenotype.

Conflict of Interest Disclosure

The authors declare not conflict of interest.

Acknowledgements

We would like to thank the animal staff at Newcastle University's Comparative Biology Centre. R.E.H. was funded by a BBSRC CASE studentship with Bruker Daltonics. J.P., T.H., J.L.M.R., and A.M were funded through a generous start-up grant of Newcastle University. A.D. and M.T. are funded through a Wellcome Trust Investigator Award (215542/Z/19/Z).

References

1. Boltz-Nitulescu G, Wiltschke C, Holzinger C, Fellinger A, Scheiner O, Gessl A, et al. Differentiation of Rat Bone Marrow Cells Into Macrophages Under the Influence of Mouse L929 Cell Supernatant. Journal of Leukocyte Biology. 1987;41(1):83–91.

2. Assouvie A, Daley-Bauer LP, Rousselet G. Growing Murine Bone Marrow-Derived Macrophages. Methods Mol Biol. 2018;1784:29–33.

3. Weischenfeldt J, Porse B. Bone Marrow-Derived Macrophages (BMM): Isolation and Applications. Cold Spring Harb Protoc. 2008 Jan 12;2008(12):pdb.prot5080.

4. Marim FM, Silveira TN, Jr DSL, Zamboni DS. A Method for Generation of Bone Marrow-Derived Macrophages from Cryopreserved Mouse Bone Marrow Cells. PLOS ONE. 2010 Dec 17;5(12):e15263.

5. Lee CM, Hu J. Cell density during differentiation can alter the phenotype of bone marrow-derived macrophages. Cell & Bioscience. 2013 Jul 29;3(1):30.

6. Fleit HB, Rabinovitch M. Interferon induction in marrow-derived macrophages: Regulation by L cell conditioned medium. Journal of Cellular Physiology. 1981 Sep 1;108(3):347–52.

7. Milhaud PG, Compagnon B, Bienvenüe A, Philippot JR. Interferon production of L929 and HeLa cells enhanced by polyriboinosinic acid-polyribocytidylic acid pH-sensitive liposomes. Bioconjug Chem. 1992 Oct;3(5):402–7.

8. Stuart PM, Zlotnik A, Woodward JG. Induction of class I and class II MHC antigen expression on murine bone marrow-derived macrophages by IL-4 (B cell stimulatory factor 1). The Journal of Immunology. 1988 Mar 1;140(5):1542–7.

9. Modolell M, Corraliza IM, Link F, Soler G, Eichmann K. Reciprocal regulation of the nitric oxide synthase/arginase balance in mouse bone marrow-derived macrophages by TH 1 and TH 2 cytokines. European Journal of Immunology. 1995;25(4):1101–4.

10. Cooper PH, Mayer P, Baggiolini M. Stimulation of phagocytosis in bone marrow-derived mouse macrophages by bacterial lipopolysaccharide: correlation with biochemical and functional parameters. The Journal of Immunology. 1984 Aug 1;133(2):913–22.

11. Zhang X, Goncalves R, Mosser DM. The isolation and characterization of murine macrophages. Curr Protoc Immunol. 2008 Nov;Chapter 14:Unit 14.1.

12. Francke A, Herold J, Weinert S, Strasser RH, Braun-Dullaeus RC. Generation of Mature Murine Monocytes from Heterogeneous Bone Marrow and Description of Their Properties. J Histochem Cytochem. 2011 Sep;59(9):813–25.

13. Cox J, Neuhauser N, Michalski A, Scheltema RA, Olsen JV, Mann M. Andromeda: A Peptide Search Engine Integrated into the MaxQuant Environment. J Proteome Res. 2011 Apr 1;10(4):1794–805.

14. Cox J, Hein MY, Luber CA, Paron I, Nagaraj N, Mann M. Accurate proteome-wide label-free quantification by delayed normalization and maximal peptide ratio extraction, termed MaxLFQ. Mol Cell Proteomics. 2014 Sep;13(9):2513–26.

15. Deutsch EW, Csordas A, Sun Z, Jarnuczak A, Perez-Riverol Y, Ternent T, et al. The ProteomeXchange consortium in 2017: Supporting the cultural change in proteomics public data deposition. Nucleic Acids Research. 2017;45(D1):D1100–6.

16. Perez-Riverol Y, Csordas A, Bai J, Bernal-Llinares M, Hewapathirana S, Kundu DJ, et al. The PRIDE database and related tools and resources in 2019: Improving support for quantification data. Nucleic Acids Research. 2019;47(D1):D442–50.

17. Trouplin V, Boucherit N, Gorvel L, Conti F, Mottola G, Ghigo E. Bone Marrow-derived Macrophage Production. J Vis Exp [Internet]. 2013 Nov 22 [cited 2019 Jan 9];(81). Available from: https://www.ncbi.nlm.nih.gov/pmc/articles/PMC3991821/

18. Mosher DF. Physiology of Fibronectin. Annual Review of Medicine. 1984;35(1):561–75.

19. Goldberg B, Green H. An Analysis of Collagen Secretion by Established Mouse Fibroblast Lines. The Journal of Cell Biology. 1964 Jul 1;22(1):227–58.

20. Schwanhäusser B, Busse D, Li N, Dittmar G, Schuchhardt J, Wolf J, et al. Global quantification of mammalian gene expression control. Nature. 2011 May;473(7347):337–42.

21. Weidinger C, Ziegler JF, Letizia M, Schmidt F, Siegmund B. Adipokines and Their Role in Intestinal Inflammation. Front Immunol. 2018;9:1974.

22. Wittamer V, Franssen J-D, Vulcano M, Mirjolet J-F, Le Poul E, Migeotte I, et al. Specific recruitment of antigen-presenting cells by chemerin, a novel processed ligand from human inflammatory fluids. J Exp Med. 2003 Oct 6;198(7):977–85.

23. Lin Y, Yang X, Yue W, Xu X, Li B, Zou L, et al. Chemerin aggravates DSS-induced colitis by suppressing M2 macrophage polarization. Cellular & Molecular Immunology. 2014 Jul;11(4):355–66.

24. Bernhagen J, Krohn R, Lue H, Gregory JL, Zernecke A, Koenen RR, et al. MIF is a noncognate ligand of CXC chemokine receptors in inflammatory and atherogenic cell recruitment. Nature Medicine. 2007 May;13(5):587–96.

25. Calandra T, Roger T. Macrophage migration inhibitory factor: a regulator of innate immunity. Nat Rev Immunol. 2003 Oct;3(10):791–800.

26. Clemente N, Raineri D, Cappellano G, Boggio E, Favero F, Soluri MF, et al. Osteopontin Bridging Innate and Adaptive Immunity in Autoimmune Diseases. J Immunol Res. 2016;2016:7675437.

27. Hughes CE, Nibbs RJB. A guide to chemokines and their receptors. FEBS J. 2018;285(16):2944–71.

28. Hashimoto S, Yamada M, Motoyoshi K, Akagawa KS. Enhancement of Macrophage Colony-Stimulating Factor–Induced Growth and Differentiation of Human Monocytes by Interleukin-10. Blood. 1997 Jan 1;89(1):315–21.

29. Lukic A, Larssen P, Fauland A, Samuelsson B, Wheelock CE, Gabrielsson S, et al. GM-CSF– and M-CSF–primed macrophages present similar resolving but distinct inflammatory lipid mediator signatures. The FASEB Journal. 2017 Jun 21;31(10):4370–81.

30. Austyn JM, Gordon S. F4/80, a monoclonal antibody directed specifically against the mouse macrophage. European Journal of Immunology. 1981;11(10):805–15.

31. Christensen JE, Andreasen SØ, Christensen JP, Thomsen AR. CD11b expression as a marker to distinguish between recently activated effector CD8+ T cells and memory cells. Int Immunol. 2001 Apr 1;13(4):593–600.

32. Collin M, McGovern N, Haniffa M. Human dendritic cell subsets. Immunology. 2013 Sep;140(1):22–30.

33. Mescher AL. Macrophages and fibroblasts during inflammation and tissue repair in models of organ regeneration. Regeneration (Oxf). 2017 Jun 6;4(2):39–53.

34. Smith RS, Smith TJ, Blieden TM, Phipps RP. Fibroblasts as sentinel cells. Synthesis of chemokines and regulation of inflammation. Am J Pathol. 1997 Aug;151(2):317–22.

35. de Brito Monteiro L, Davanzo GG, de Aguiar CF, Corrêa da Silva F, Andrade JR de, Campos Codo A, et al. M-CSF- and L929-derived macrophages present distinct metabolic profiles with similar inflammatory outcomes. Immunobiology. 2020 May;225(3):151935.

36. Reyes JL, Terrazas LI, Espinoza B, Cruz-Robles D, Soto V, Rivera-Montoya I, et al. Macrophage Migration Inhibitory Factor Contributes to Host Defense against Acute Trypanosoma cruzi Infection. Infection and Immunity. 2006 Jun 1;74(6):3170–9.

Supplementary Figures

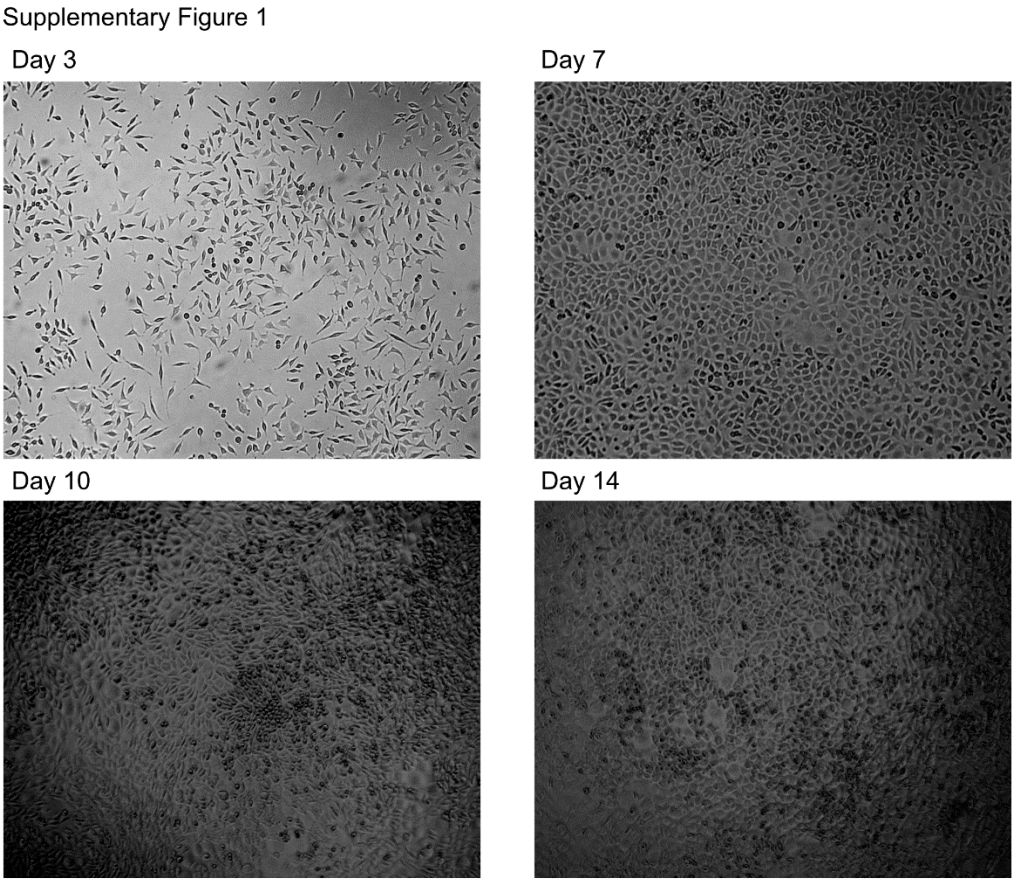

Supplementary Figure 1: **Brightfield light microscopy images of L929 cells.** Brightfield light microscopy images of L929 fibroblasts at the secretome time points showing significant changes in morphology with increasing confluency.

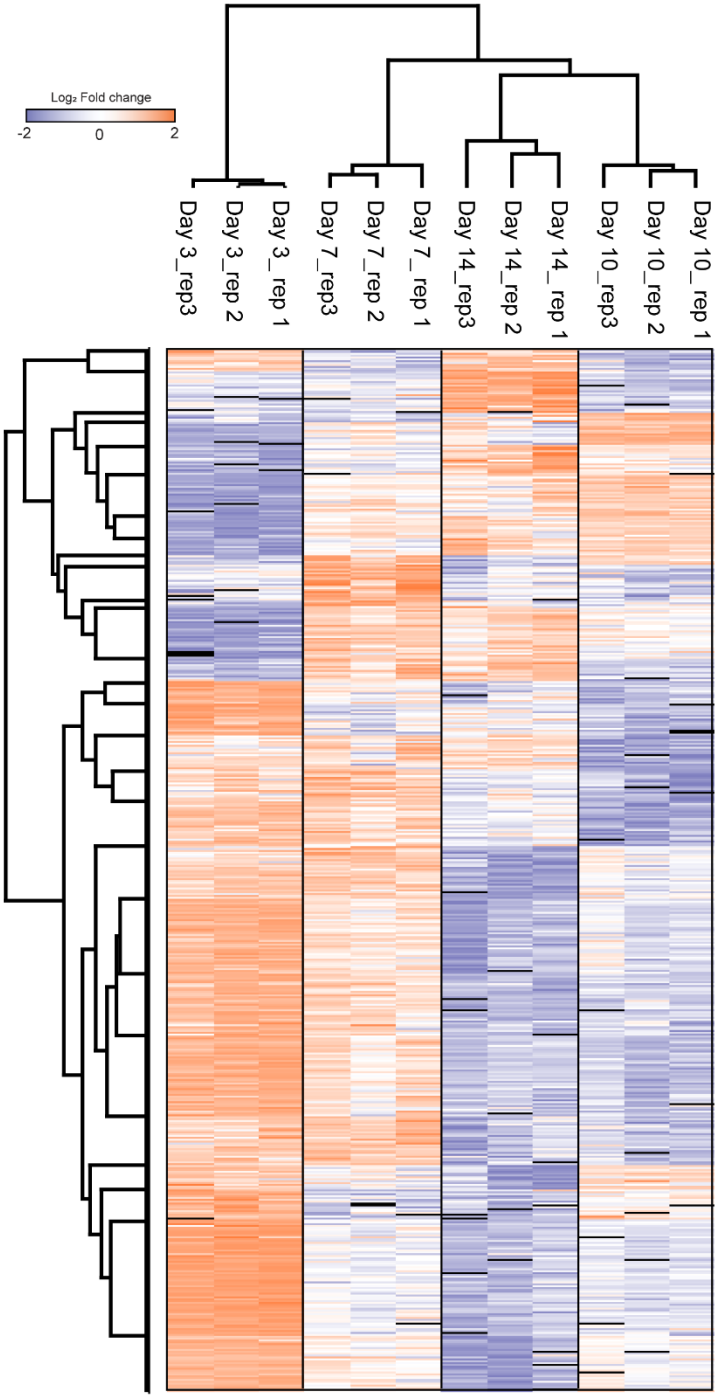

Supplementary Figure 2: **Correlation clustering of all secretome experiments shows high reproducibility between replicates.**

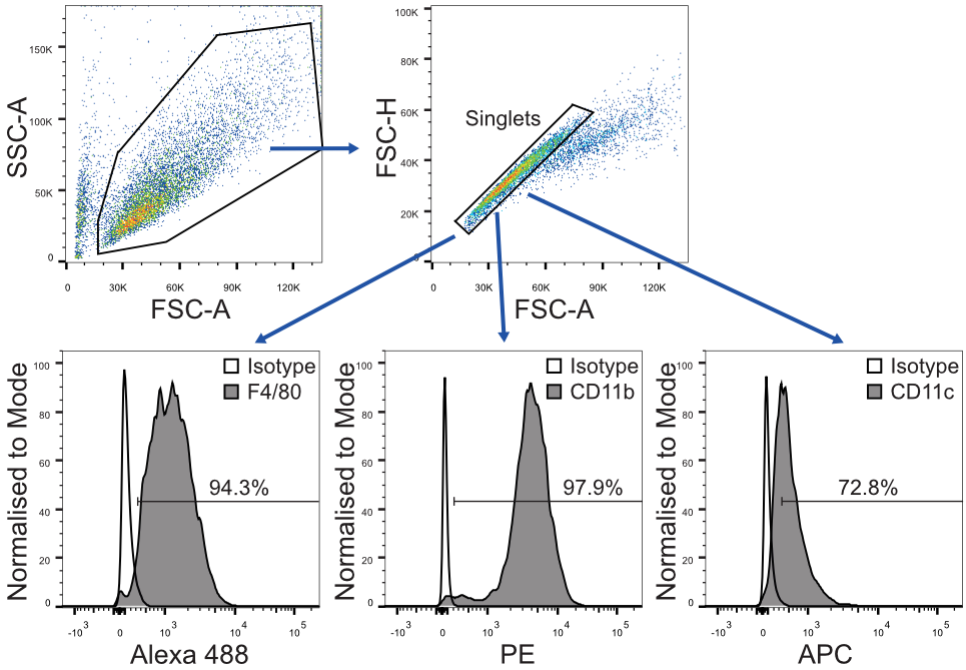

Supplementary Figure 3 **Flow cytometry analysis workflow.** BMDMs were selected based on SSC-A/FSC-A properties. Singlets were gated as FSC-H/FSC-A, then Alexa 488, PE and APC negative and positive population using the corresponding isotypes antibodies. The percentage of positive cells for each antibody was determined based on gates drawn for each isotype control.